



TITLE:

Effects of Metal Hydride Coatings at the Electrodes on Neutron Production Rate in a Discharge-Type Fusion Neutron Source

AUTHOR(S):

Sakabe, T.; Kenjo, S.; Ogino, Y.; Mukai, K.; Bakr, M.; Yagi, J.; Konishi, S.

CITATION:

Sakabe, T. ...[et al]. Effects of Metal Hydride Coatings at the Electrodes on Neutron Production Rate in a Discharge-Type Fusion Neutron Source. IEEE Transactions on Plasma Science 2022, 50(11): 4500-4505

ISSUE DATE:

2022-11

URL:

<http://hdl.handle.net/2433/277554>

RIGHT:

© 2022 IEEE. Personal use of this material is permitted. Permission from IEEE must be obtained for all other uses, in any current or future media, including reprinting/republishing this material for advertising or promotional purposes, creating new collective works, for resale or redistribution to servers or lists, or reuse of any copyrighted component of this work in other works.; This is not the published version. Please cite only the published version. この論文は出版社版ではありません。引用の際には出版社版をご確認ください。

Effects of metal hydride coatings at the electrodes on neutron production rate in a discharge-type fusion neutron source

T. Sakabe, S. Kenjo, Y. Ogino, K. Mukai, M. Bakr, J. Yagi, and S. Konishi

Abstract—A glow discharge fusion neutron source that utilizes nuclear fusion reactions of deuterium has been upgraded. The fusion reactions in this device mainly occur by collisions between the charged or neutral particles and the hydrogen isotopes trapped at the surface of electrodes. In addition, it is known that the metal hydride coating on the electrode enhances the neutron production rate (NPR). Therefore, the elemental distribution, including deuterium, in the depth direction on the electrode is an essential factor in neutron production. However, the distribution on the electrode has not been experimentally investigated. This study aims to analyze the distribution experimentally and indicate the effect of the metal hydride coatings. To achieve this purpose, we prepared the titanium (Ti) - coated cathode and the uncoated cathode, of which the base material was stainless steel. After that, the neutron production test was performed in the range of from 5 to 40 mA currents and from 20 to 60 kV applied voltage. This test indicated that the NPR was improved by coating the cathode with Ti than the uncoated cathode. Additionally, depth profiling on the cathodes by glow discharge optical emission spectrometry (GD-OES) was performed. While the analysis indicated the concentration of deuterium on both cathodes was increased after the test, there was no significant difference in the concentration of deuterium between both cathodes. Furthermore, the concentration of Ti on the Ti-coated cathode was vastly decreased. The cause of these changes needs to be investigated.

Index Terms— fusion reaction, glow discharge, neutron source, metal hydride coating

I. INTRODUCTION

The discharge-type neutron source is a compact system that causes the deuterium-deuterium fusion reaction by inducing a glow discharge [1]. The applications of the discharge-type fusion neutron source are not limited to fusion research purposes [2] but extended to also in other fields such as land mine detection [3], and cancer therapy [4] have been studied. Furthermore, the operation which utilizes the deuterium-tritium fusion reaction is expected to achieve a higher neutron production rate (NPR) because of the higher fusion reaction cross-section. Thus, the experiment using tritium was conducted for an increasing number of applications [5]. In a recent publication, the self-sufficient system for

reducing the amount of hydrogen isotope fuel gas is proposed to accomplish the deuterium-tritium operation [6].

The configuration consists of the transparent cathode and the vacuum chamber that serves as the anode. The chamber is filled with deuterium gas during the operation time. By applying a high voltage between the electrodes, ions are generated through glow discharge. These ions are accelerated by an electric field and gain high energy. These ions induce the atomic and molecular processes, such as ionization, dissociation, interchange reaction, etc. [7]. Consequently, the nuclear fusion reaction is caused by the ions and the neutral particles, which have the energies required for the reaction.

Different kinds of collisions induce the fusion reaction inside the chamber. In the original concept, the collisions between the energetic ions, known as the beam-beam reaction, were expected to be dominant. However, this kind of collision is negligible at less than 100 mA [8]. On the other hand, the collisions between the energetic ions and the background gas are not negligible under broader operating conditions. Furthermore, in recent publications, the contribution of the collisions between the energetic particles and the hydrogen isotopes trapped on the electrodes has been indicated.

The prior studies experimentally measured the contribution of the fusion reaction on the electrode surface. Though no material dependence of cathode was observed in the experiments using the grid cathode with a very low surface area [9], the improvement in NPR was observed in the experiment using the electrodes made of a material that retains hydrogen isotopes [10-12]. In addition, the simulations which calculated atomic and molecular processes with the Monte Carlo collision scheme also indicated the contribution of the fusion reaction that occurred on the electrode [13]. Moreover, the prior study showed that when the metal hydride coating was applied to the cylindrical type, an enhancement of the NPR was confirmed [13].

Hence, in the discharge-type neutron source, the metal hydride coating on the electrode is considered a promising method for enhancing the fusion reaction on the electrodes. Additionally, the idea of using a hydride-forming material for the coating and material that meets the required specifications

This work was supported by a Grant-in-Aid for young scientists (20K14442) from the Japan Society for the Promotion of Science (JSPS).

T. Sakabe, S. Kenjo, and Y. Ogino are with the Graduate School of Energy Science, Kyoto University, Kyoto 611-0011, Japan. (e-mail: sakabe.toshiro.74n@st.kyoto-u.ac.jp)

K. Mukai, J. Yagi, M. Bakr and S. Konishi are with the Institute of Advanced Energy, Kyoto University, Kyoto 611-0011, Japan. M. Bakr is now at the physics department, Assiut University 71516 Egypt.

Color versions of one or more of the figures in this article are available online at <http://ieeexplore.ieee.org>

for the electrodes as the base material can be proposed. The advantage of this idea is that an electrode that has both advantages can be developed. The specifications required for electrodes include high thermal capacity, high mechanical strength, low electrical resistance, etc.

Accordingly, the elemental distribution in the depth direction on the electrode, including hydrogen isotopes, is vital in terms of neutron production. However, the distribution has not been experimentally investigated before and after the neutron production test. This study aims to analyze the distribution experimentally and indicate the effect of the metal hydride coatings. To this end, the neutron production test using the spherical chamber was conducted by employing a cathode subjected to a titanium (Ti) coating that forms a hydride. Our experiment compared two cathodes; the Ti-coated cathode and the uncoated cathode. In addition, depth profiling on the cathodes was conducted to investigate the elemental distribution before and after the neutron production test by glow discharge optical emission spectroscopy (GD-OES) [14]. In this paper, the results of the neutron production test and the depth profile are shown. Finally, the effects of the coating and its prospects are discussed.

II. METHODS

A. Cathodes preparation

This study prepared two cathodes: the Ti-coated cathode and the uncoated cathode. The cathodes were assembled by combining the ring-shaped plates. Fig. 1 (a) shows the plates for the cathodes. The outer and inner diameter of the ring was 8 cm and 4 cm, respectively. The width of the ring was 2 cm. The thickness of the plate was 1 mm. The base material of the cathode was stainless steel (SUS304).

As a pretreatment, the plates were polished with emery paper. Subsequently, the plates were soaked in acetone and cleaned for 30 minutes using an ultrasonic cleaning device.

To coat Ti on the ring-shaped plates, vacuum vapor deposition was adapted. The vapor deposition system is described in Fig. 2. The Ti alloy rod (ULVAC, Inc., PGT-3F), manufactured initially as a part of a getter pump, installed inside the chamber was the source of Ti vapor. In this process, after the chamber was drawn to 10^{-2} Pa order or less, the current heating of the filament was started. The electric input was direct current power, and the heating current was 40 A. The heating time for vapor deposition of each surface was 75 minutes. The sample plates (about 2 cm x 2 cm) made of SUS304 were coated simultaneously during the deposition process. The sample plates were employed to measure the elemental distribution on the coating surface.

After the vapor deposition, a ring-shaped plate was combined using a spot welder to form a shape that can be used as a cathode. Fig. 1 (b) shows the Ti-coated cathode after assembly.

B. Neutron production test

The neutron production test was conducted by using the spherical chamber. The test system is described in Fig. 3. The prepared cathode was installed inside the spherical chamber. The cathode was biased to negative high voltage via the feedthrough system. The spherical chamber was grounded and

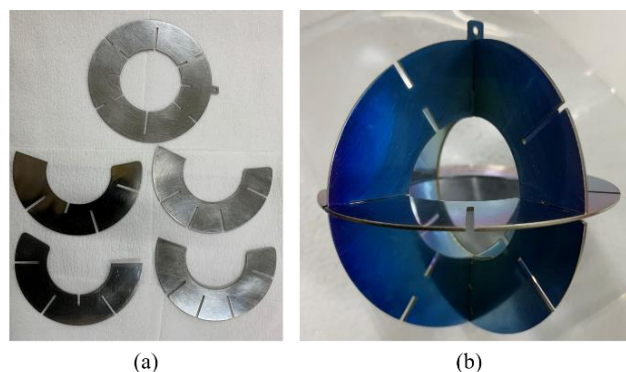


Fig. 1. The SUS304 plates for cathodes (a), and the Ti-coated cathode after assembly (b)

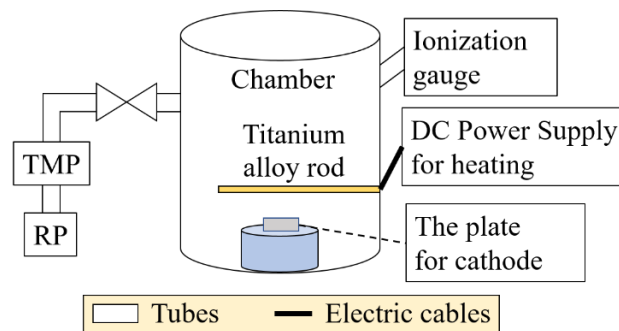


Fig. 2. The diagram of the vapor deposition system. TMP and RP denote a turbo molecular pump and a rotary pump.

served as the anode. The inner diameter of the chamber was 25 cm. The water layer, which width was 5 cm, existed around the internal space of the chamber. The water chiller circulated water to cool the inner wall keeping the water temperature at 10 °C. The pressure inside the chamber was measured by an ionization gauge. A ^3He proportional counter measured neutrons.

After drawing a vacuum to 10^{-2} Pa order or less by a turbo molecular pump and a rotary pump, high voltage was applied between the cathode and the anode. While the high voltage was applied in a vacuum, deuterium gas was introduced to the chamber, and a glow discharge started. The gas pressure was controlled by adjusting the amount of the gas flow with the mass flow controller to keep the voltage. The operation mode of the power supply was a constant current mode.

The voltage conditions were set in increments of 5 kV in the range of 20 to 60 kV. The current requirements were put in increments of 5mA in 5 to 40mA. The test was conducted by changing the sequence conditions from low voltage to high voltage conditions. For each voltage condition, the current conditions were altered from low to high current conditions. In addition, the measurement of neutrons was performed three times at each electric condition.

C. Depth profiling

Each thickness of the Ti-layer and the elemental distribution in the depth direction of the cathodes was obtained by glow

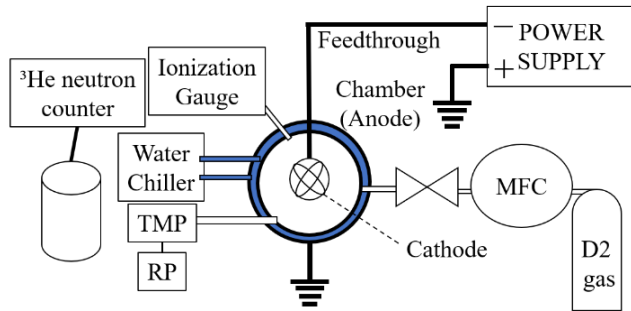


Fig. 3. The system diagram of the neutron production test. MFC, TMP, and RP denote a mass flow controller, a turbo molecular pump, and a rotary pump.

discharge optical emission spectroscopy (GD-OES) (GD-profiler2, HORIBA, Ltd.) before and after the neutron production test. Firstly, the Ti-coated sample was used to calculate the scan speed of GD-OES in the depth direction. The depth of the scan part was measured by atomic force microscope (AFM) (VN-8010, KEYENCE CORPORATION). The depth was divided by the operation time of GD-OES to calculate the scan speed. In this process, the scan speed turned out to be 121.5 nm/s. This calculation process is based on the assumption that the rate had been constant throughout the operation time.

The scan speed was 121.5 nm/s, and the measurement time was 30 seconds. Thus, the measurement depth was about 3.6 μm . The diameter of the measurement point was about 4 mm. Before the neutron production test, the Ti-coated plate and the SUS304 plate were measured by GD-OES. Since GD-OES is a destructive inspection that scrapes a sample's surface, the sample plate was employed to measure the Ti-coated surface instead of the Ti-coated cathode. After the neutron production test, the cathodes were removed from the spherical chamber and cut into fragments for the measurement by GD-OES. After that, depth profiling for the surface of each cathode was conducted.

III. RESULTS

A. Neutron production test

Figs. 4 and 5 show the result of the neutron production test. It can be seen from the figures that the NPR in the case of the Ti-coated cathode surpassed that of the uncoated cathode. The

TABLE I
THE AVERAGE VALUE OF THE INCREASING RATIO UNDER EACH VOLTAGE CONDITION, WITH THE STANDARD ERROR.

Voltage (kV)	The increasing ratio
20	1.40 ± 0.29
25	1.42 ± 0.065
30	1.39 ± 0.045
35	1.30 ± 0.035
40	1.47 ± 0.027
45	1.44 ± 0.011
50	1.31 ± 0.0085
55	1.33 ± 0.0071
60	1.30 ± 0.0046

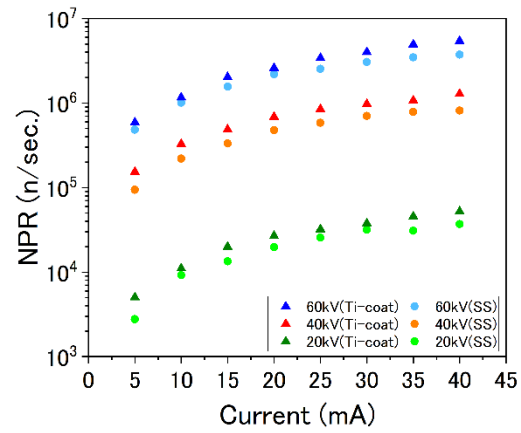


Fig. 4. Comparison of the NPR for the uncoated cathode and the Ti-coated cathode as a function of current.

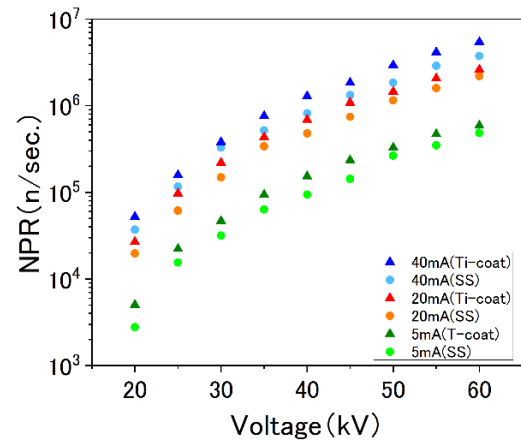


Fig. 5. Comparison of the NPR for the uncoated cathode and the Ti-coated cathode as a function of voltage.

increasing ratio is defined as the ratio of the NPR in the case of the Ti-cathode to the NPR in the case of the uncoated cathode. The average value of the increasing ratio for each voltage and current condition ranged from 1.30 to 1.48, as shown in Tables I and II. The rising ratio has no dependence on the voltages and currents. At 2.4 kW (60kV, 40mA) of maximum electric input in this test, the NPR of the Ti-coated cathode was $(5.44 \pm 0.034) \times 10^6$ n/s, and that of the uncoated cathode was $(3.75 \pm 0.020) \times 10^6$ n/s. For the uncoated cathode, the gas pressure during the

TABLE II
THE AVERAGE VALUE OF THE INCREASING RATIO UNDER EACH CURRENT CONDITION, WITH THE STANDARD ERROR.

Current (mA)	The increasing ratio
5	1.48 ± 0.21
10	1.35 ± 0.071
15	1.35 ± 0.068
20	1.37 ± 0.030
25	1.32 ± 0.035
30	1.32 ± 0.038
35	1.37 ± 0.018
40	1.43 ± 0.025

measurement was within the range of 2.4 to 3.6 Pa, while for the Ti-coated cathode, the pressure was higher than 5 Pa in most conditions.

Additionally, the NPR tended to increase proportionally to the current and exponentially to the voltage regarding both cathodes. However, as the voltage grew, the NPR became less than this tendency, as shown in Fig. 5.

B. Depth profiling of the uncoated cathode

Fig. 6-A shows the depth profiling result of SUS304 before the neutron production test. Iron and chromium, which were constituents of SUS304, dominated at depths of about 0.5 μm and deeper. The intensity of oxygen was the largest on the outermost surface. As shown in Fig. 6-B, after the neutron production test, the intensity of deuterium was increased. Additionally, there were no significant changes in the other values of intensity.

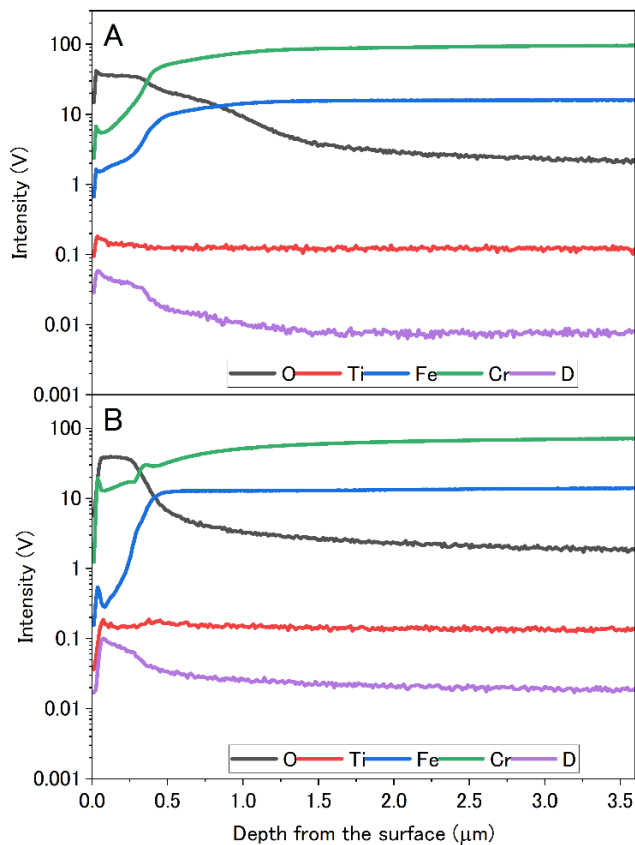


Fig. 6. GD-OES depth profiling of SUS304 before the neutron production test (A). GD-OES depth profiling of the uncoated cathode after the neutron production test (B).

C. Depth profiling of the Ti-coated cathode

Fig. 9-A shows the depth profiling result of the Ti-coated surface of the sample. The thickness of the Ti layer was about 0.7 μm from the surface. On the other hand, the penetration range of 60-keV deuterium ions, which was assumed to be the maximum energy in this study, was calculated to be about 0.5 μm by TRIM [15]. Therefore, this thickness was enough to capture 60-keV deuterium ions inside the Ti layer. In addition,

iron and chromium dominated at the more profound point of the Ti layer. After the neutron production test, the appearance of the Ti-coated cathode was changed, as shown in Fig. 7. The color of the cathode was blue before the neutron production test. However, the cathode part was exposed to the gas, and other particles changed to dark brown or silver. There were color gradations between the dark brown part and the silver part. The welded portion of the cathode, where the two plates overlapped and did not touch gasses and other particles inside the chamber, remained blue, as shown in Fig. 7 (c).

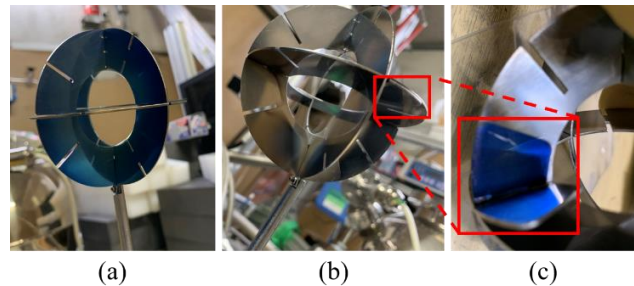


Fig. 7. The Ti-coated cathode before the neutron production test (a), the Ti-coated cathode after the neutron production test (b), the welded part of the Ti-coated cathode after the neutron production test (c).

Fig. 8 presents the measurement point of the Ti-coated cathode by GD-OES. The round marks are the spots that were scratched by the GD-OES inspection. The parts marked 1, 2, and 3 in Fig. 8 are the dark brown part, the silver part, and the blue region, respectively. Fig. 9 shows the depth profiling results of the Ti-coated cathode before and after the neutron

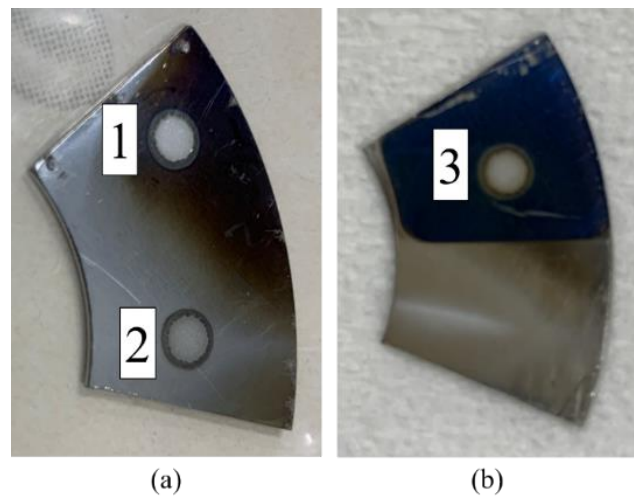


Fig. 8. The measurement points of the Ti-coated cathode by GD-OES. These fragments were cut for measurement after the neutron production test (a, b). The dark brown part and the blue part (a), the blue part (b). No.1, No.2, and No.3 in this figure correspond to B, C, and D in Fig. 9, respectively.

production test. The concentration of Ti within 0.5 μm from the surface decreased at all three measurement points after the test.

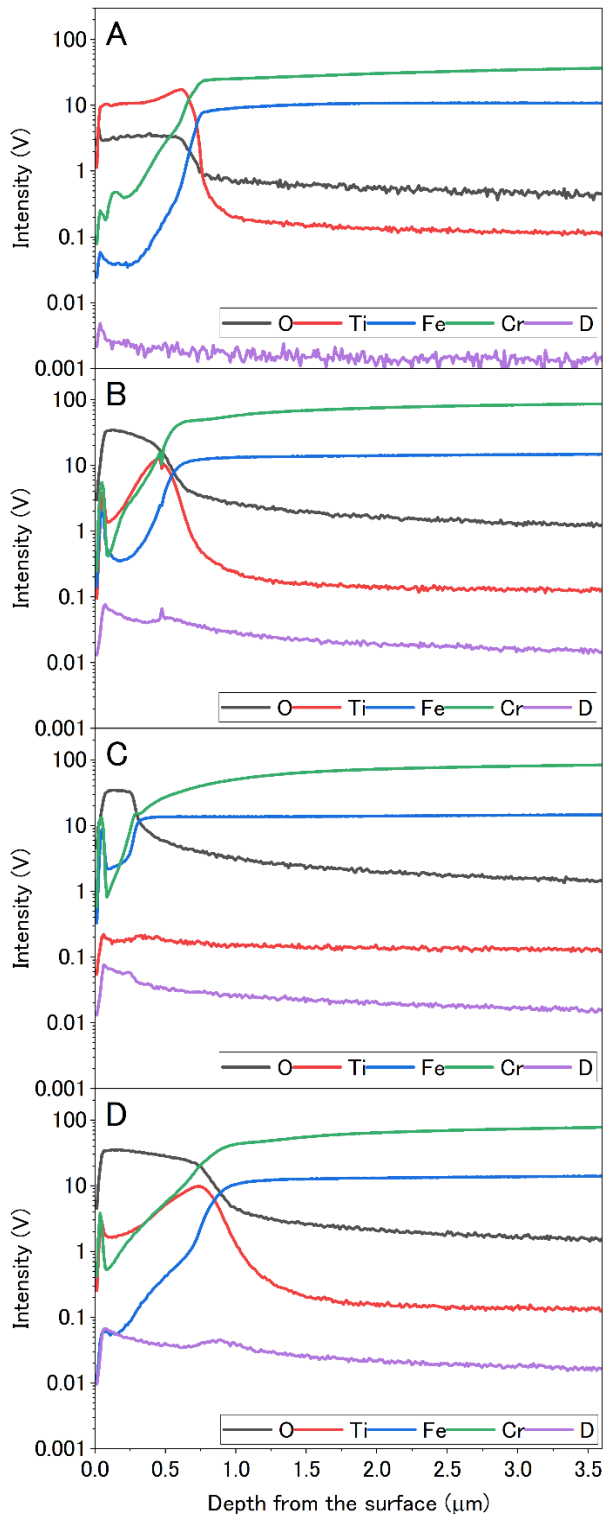


Fig. 9. GD-OES depth profiling of the Ti-coated sample plate before the neutron production test (A). GD-OES depth profiling of the Ti-coated sample plate after the neutron production test (B, C, D). B, C, and D correspond to No.1, No.2, and No.3 in Fig. 8.

Significantly, the intensity of Ti at the silver part was equivalent

to that of the SUS304 plate. The intensity of deuterium at the measurement points increased by about one order of magnitude after the neutron production test throughout the entire measurement range, as with the uncoated cathode, iron, and chromium, which were constituents of SUS304, dominated at depths of about 1.0 μm and deeper.

IV. DISCUSSION

A. Neutron production test

In the prior study, the increasing ratio of the NPR as a function of cathode voltage between pure Ti and stainless steel cathodes ranged from 1.36 to 1.64 in an applied voltage range from 20 to 70kV [11]. On the other hand, the increasing ratio in this study between two cathodes ranged from 1.30 to 1.48, which is the same level as the prior study. As the experimental system was the same as the initial study [11] except for the cathode, it is suggested that the metal hydride coating on the electrodes coating with the metal hydride coating might have comparable performance to the electrodes made of the pure metal forming the hydride.

The dependence of NPR on voltage and current is consistent with previous studies [10], [11] regarding both cathodes. However, as the voltage was increased, the NPR became smaller than this tendency. This result might be due to the increase in the temperature of the cathodes as the electric input power increases. For example, in the case of the prior study [11] using the spherical cathode, the temperature of the stainless steel cathode was 860 ± 3 °C at 2.4 kW (30 kV, 80 mA). In addition, another prior study indicates that as the cathode temperature rises, the desorption of hydrogen gas from the cathode progresses, and the NPR gain decreases [16]. Therefore, it is possible that the deuterium on the surface desorbed according to the temperature characteristics of the material [17], and the NPR gain decreased. To clarify the cause of this tendency, it is necessary to measure the temperature of the cathode. Furthermore, for the Ti-coated cathode, considering the GD-OES results, it is possible that the Ti on the surface gradually decreased during the operation, and the NPR decreased accordingly.

B. Depth profiling

After the neutron production test, the concentration of Ti in the Ti-coated cathode was decreased. There was no difference in the measurement value of Ti at depths greater than 2 μm between the results of the uncoated cathode (Fig. 6) and the Ti-coated cathode (Fig. 9). Therefore, it is considered that thermal diffusion of Ti into SS did not occur. In addition, there was a significant difference in the decrease of Ti between the welded part and the other part. Therefore, it is suggested that the ions, electrons, and neutral particles in the chamber collided with the cathode surface except for the welded portion, and Ti on the surface was removed. In addition, considering the literature value of vapor pressure [18], it is unlikely that most Ti vaporized and was removed from the surface.

Furthermore, the concentration of deuterium increased at both cathodes. There was no significant difference in deuterium concentration between the uncoated cathode and the Ti-coated

cathode results. This may be due to the decrease in Ti on the Ti-coated cathode.

V. CONCLUSION

We indicated the effect of the metal hydride coating. In this study, the Ti coating was applied to the cathode as the metal hydride coating, and the improvement of the NPR was confirmed. The increasing ratio was at the same level as the previous study compared the pure Ti cathode and the SS cathode. Thus, it is suggested that the metal hydride coating can be an effective method to achieve NPR, which is equivalent to the case using pure metal. In addition, as mentioned in the introduction section, it was found that an electrode that has both advantages of coating material and base material can be fabricated by applying a metal hydride coating.

However, this study also indicates that the effect of the coating might decrease gradually during long-term operation. In order to establish the coating method for the electrode, robustness is the essential factor, and it is necessary to clarify the cause of the decrease in Ti.

REFERENCES

- [1] G. H. Miley, and J. Sved, "The IEC - A plasma-target-based neutron source," *Applied Radiation and Isotopes*, vol. 48, no. 10-12, pp. 1557-1561, Oct-Dec, 1997, doi: [10.1016/S0969-8043\(97\)00257-1](https://doi.org/10.1016/S0969-8043(97)00257-1).
- [2] K. Mukai, Y. Ogino, M. I. Kobayashi, M. Bakr, J. Yagi, K. Ogawa, M. Isobe, and S. Konishi, "Evaluation of tritium production rate in a blanket mock-up using a compact fusion neutron source," *Nuclear Fusion*, vol. 61, no. 4, Apr, 2021, doi: [10.1088/1741-4326/abe4e7](https://doi.org/10.1088/1741-4326/abe4e7).
- [3] G. L. Kulcinski, J. F. Santarius, K. Johnson, A. Megahed, and R. L. Bonomo, "Identification of Landmines and IEDs Using Compact Fusion Neutron Sources on Drones," *Fusion Science and Technology*, vol. 72, no. 3, pp. 455-460, 2017, doi: [10.1080/15361055.2017.1333862](https://doi.org/10.1080/15361055.2017.1333862).
- [4] Y. Nakai, K. Noborio, Y. Takeuchi, R. Kasada, Y. Yamamoto, and S. Konishi, "A Feasibility Study of an Application of Fusion Neutron Beam Source Based on Cylindrical Discharge Device for Cancer Therapy," *Fusion Science and Technology*, vol. 64, no. 2, pp. 379-383, Aug 2013, doi: [10.13182/FST13-A18106](https://doi.org/10.13182/FST13-A18106).
- [5] M. Ohnishi, Y. Yamamoto, H. Osawa, Y. Hatano, Y. Torikai, I. Murata, K. Kamakura, M. Onishi, K. Miyamoto, H. Konda, K. Masuda, and E. Hotta, "Tritium burning in inertial electrostatic confinement fusion facility," *Fusion Engineering and Design*, vol. 109, pp. 1709-1713, Nov, 2016, doi: [10.1016/j.fusengdes.2015.10.025](https://doi.org/10.1016/j.fusengdes.2015.10.025).
- [6] S. Kenjo, Y. Ogino, K. Mukai, M. Bakr, J. Yagi, and S. Konishi, "Employing of ZrCo as a fuel source in a discharge-type fusion neutron source operated in self-sufficient mode," *International Journal of Hydrogen Energy*, vol. 47, no. 5, pp. 3054-3062, Jan, 2022, doi: [10.1016/j.ijhydene.2021.10.250](https://doi.org/10.1016/j.ijhydene.2021.10.250).
- [7] D. R. Boris, and G. A. Emmert, "Composition of the source region plasma in inertial electrostatic confinement devices," *Physics of Plasmas*, vol. 15, no. 8, Aug 2008, doi: [10.1063/1.2965148](https://doi.org/10.1063/1.2965148).
- [8] K. Noborio, Y. Yamamoto, Y. Ueno, and S. Konishi, "Confinement of ions in an inertial electrostatic confinement fusion (IECF) device and its influence on neutron production rate," *Fusion Engineering and Design*, vol. 81, no. 8-14, pp. 1701-1705, Feb, 2006, doi: [10.1016/j.fusengdes.2005.09.013](https://doi.org/10.1016/j.fusengdes.2005.09.013).
- [9] A. L. Wehmeyer, R. F. Radcliff, and G. L. Kulcinski, "Optimizing neutron production rates from D-D fusion in an inertial electrostatic confinement device," *Fusion Science and Technology*, vol. 47, no. 4, pp. 1260-1264, May 2005, doi: [10.13182/FST05-A861](https://doi.org/10.13182/FST05-A861).
- [10] M. Bakr, K. Masuda, and M. Yoshida, "Improvement of the Neutron Production Rate of IEC Fusion Device by the Fusion Reaction on the Inner Surface of the IEC Chamber," *Fusion Science and Technology*, vol. 75, no. 6, pp. 479-486, 2019, doi: [10.1080/15361055.2019.1609821](https://doi.org/10.1080/15361055.2019.1609821).
- [11] M. Bakr, J. P. Wulfkuhler, K. Mukai, K. Masuda, M. Tajmar, and S. Konishi, "Evaluation of 3D printed buckyball-shaped cathodes of titanium and stainless-steel for IEC fusion system," *Physics of Plasmas*, vol. 28, no. 1, Jan 2021, doi: [10.1063/5.0033342](https://doi.org/10.1063/5.0033342).
- [12] R. Bowden-Reid, J. Khachan, J.-P. Wulfkuhler, and M. Tajmar, "Evidence for surface fusion in inertial electrostatic confinement devices," *Physics of Plasmas*, vol. 25, no. 11, Nov, 2018, doi: [10.1063/1.5053616](https://doi.org/10.1063/1.5053616).
- [13] K. Noborio, Y. Yamamoto, and S. Konishi, "Neutron production rate of inertial electrostatic confinement device with fusion reaction on the surface of electrodes," *Fusion Science and Technology*, vol. 52, no. 4, pp. 1105-1109, Nov 2007, doi: [10.13182/FST07-A1645](https://doi.org/10.13182/FST07-A1645).
- [14] M. Wilke, G. Teichert, R. Gemma, A. Pundt, R. Kirchheim, H. Romanus, and P. Schaaf, "Glow discharge optical emission spectroscopy for accurate and well resolved analysis of coatings and thin films," *Thin Solid Films*, vol. 520, no. 5, pp. 1660-1667, Dec, 2011, doi: [10.1016/j.tsf.2011.07.058](https://doi.org/10.1016/j.tsf.2011.07.058).
- [15] J. F. Ziegler, M. D. Ziegler, and J. P. Biersack, "SRIM - The stopping and range of ions in matter (2010)," *Nuclear Instruments & Methods in Physics Research Section B-Beam Interactions with Materials and Atoms*, vol. 268, no. 11-12, pp. 1818-1823, Jun, 2010, doi: [10.1016/j.nimb.2010.02.091](https://doi.org/10.1016/j.nimb.2010.02.091).
- [16] R. Bowden-Reid, and J. Khachan, "An inertial electrostatic confinement fusion system based on graphite," *Physics of Plasmas*, vol. 28, no. 4, pp. 7, Apr 2021, doi: [10.1063/5.0038766](https://doi.org/10.1063/5.0038766).
- [17] Y. Yagodzinskyy, O. Todoshchenko, S. Papula, and H. Hanninen, "Hydrogen Solubility and Diffusion in Austenitic Stainless Steels Studied with Thermal Desorption Spectroscopy," *Steel Research International*, vol. 82, no. 1, pp. 20-25, Jan 2011, doi: [10.4028/www.scientific.net/DDF.258-260.322](https://doi.org/10.4028/www.scientific.net/DDF.258-260.322).
- [18] C. B. Alcock, V. P. Itkin, and M. K. Horrigan, "Vapor-Pressure Equations For The Metallic Elements - 298-2500-K," *Canadian Metallurgical Quarterly*, vol. 23, no. 3, pp. 309-313, 1984, doi: [10.1179/cmqr.1984.23.3.309](https://doi.org/10.1179/cmqr.1984.23.3.309).